JPEDAV (2008) 29:2–10
DOI: 10.1007/s11669-007-9238-z
1547-7037 ©ASM International

Computational Study of Atomic Mobility for fcc Phase of Co-Fe and Co-Ni Binaries

Y.-W. Cui, M. Jiang, I. Ohnuma, K. Oikawa, R. Kainuma, and K. Ishida

(Submitted April 27, 2007; in revised form August 10, 2007)

Abundant experimental diffusion data in two Co-base binary systems, that is, Co-Ni and Co-Fe, have been assessed to develop the atomic mobility for the face-centered cubic (fcc) phase of the two binaries. The general agreement is obtained by comprehensive comparisons made between the calculated and experimental diffusion coefficients. The developed mobility database, in conjunction with the CALPHAD-type thermodynamic description, has been successfully used to simulate such typical experimental interdiffusion phenomena as the concentration profiles, the microstructural stability of the Kirkendall plane, and the lattice plane displacement.

Keywords binary diffusion, critical assessment, DICTRA modeling, Kirkendall effect

1. Introduction

Very recently, cobalt-base alloys were found to offer great promise as candidates for next-generation high-temperature materials.[1] The diffusion process, as for Ni-base superalloys, is expected to govern much of heat treatment processing and performance of Co-base high-temperature alloys. The composition and morphology of the ordered face-centered cubic (fcc) precipitate γ' are also dependent on the diffusion interaction between γ' and the disordered fcc matrix γ. Knowledge of both thermodynamics and diffusion characteristics is critically important in developing an understanding of this new type of Co-base high-temperature alloys. As the CALPHAD technique (Calculation of Phase Diagram) has made significant progress in technological applications, there is no longer a problem finding an appropriate thermodynamic description for a specific constituent binary system of the Co-base alloys; for instance, there is such data for the Co-Ni system,[2] the Co-Fe system,[3] and the Co-W system.[4] While an atomic mobility database has recently been developed for the fcc phase of multicomponent Ni-base superalloys,[5,6] no work has yet been reported for Co-base high-temperature alloys. In contrast, practical modeling algorithms, with the phase field model as representative,[7-9] can at present realistically model the microstructural evolution of certain materials with input of real variable mobility. As a consequence, there is an increasing need for accurate expressions of atomic mobility.

The DICTRA code (DIffusion Controlled TRAnsformation), running with data for atomic mobility, is capable of modeling diffusion-limited phenomena for multicomponent alloys.[10] The atomic mobility database developed in this code, in conjunction with the CALPHAD-based thermodynamics, not only permits prediction of the concentration profile determined from diffusion-couple experiments, but also enables analysis of the microstructural stability of the Kirkendall plane and the lattice plane displacement.[11,12] Accordingly, the purpose of the present work, as the first part of development of an atomic mobility database for multicomponent Co-base high-temperature alloys, is to assess the atomic mobility for the fcc phase of two fundamental Co-base binaries, that is, Co-Ni and Co-Fe, and provide further insight into their diffusion characteristics by simulating in-depth diffusion behaviors resulting from interdiffusion.

Y.-W. Cui, M. Jiang, I. Ohnuma, K. Oikawa, and **K. Ishida,** Department of Materials Science, Graduate School of Engineering, Tohoku University, Sendai 980-8579, Japan; **Y.-W. Cui, K. Oikawa, R. Kainuma,** and **K. Ishida,** Core Research for Evolutional Science and Technology (CREST), Japan Science and Technology Agency (JST), Saitama, Japan; **M. Jiang,** Department of Materials Science, College of Materials and Metallurgy, Northeastern University, Shenyang 110004, China; and **R. Kainuma,** Institute of Multidisciplinary Research for Advanced Materials (IMRAM), Tohoku University, Sendai 980-8577, Japan. Contact e-mail: ycui@material.tohoku.ac.jp.

2. Modeling

2.1 Atomic Mobility and Diffusivity

Andersson and Agren[13] suggested that the atomic mobility M_i of species i could be expressed as a function of temperature T,

$$M_i = M_i^0 \exp\left(\frac{-Q_i^S}{RT}\right)\frac{1}{RT} \qquad \text{(Eq 1)}$$

where Q_i^S is the activation energy, M_i^0 is the frequency factor, and R is the gas constant. Note that the mobility parameters in the DICTRA notation, $-Q_i^S$ and $RT \ln M_i^0$, can be grouped into one single parameter, $Q_i = -Q_i^S + RT \ln M_i^0$, in the case when there is no magnetic effect on the atomic mobility. Similar to the phenomenological CALPHAD technique, the parameter Q_i is assumed

to be composition dependent[14] and can be expressed by a Redlich-Kister polynomial in composition,

$$\mathrm{Q}_i = \sum_p x_p \mathrm{Q}_i^p + \sum_p \sum_{q>p} x_p x_q \left[\sum_{r=0,1,2,\ldots} {}^r\mathrm{Q}_i^{p,q} (x_p - x_q)^r \right] + \sum_p \sum_{q>p} \sum_{v>q} x_p x_q x_v \left[v_{pqv}^s {}^s\mathrm{Q}_i^{p,q,v} \right], \quad (s = p, q, v), \tag{Eq 2}$$

where x_p is the mole fraction of species p, Q_i^p is the value Q_i of species i in pure species p, ${}^rQ_i^{p,q}$ and ${}^sQ_i^{p,q,v}$ are the binary and ternary interaction parameters, and the parameter v_{pqv}^s is given by $v_{pqv}^s = x_s + (1 - x_p - x_q - x_v)/3$. The tracer diffusion coefficient D_i^* is rigorously related to the atomic mobility by a simple relation, $D_i^* = RTM_i$. The interdiffusion coefficient with n as dependent species, $\tilde{D}_{pq}^n$, can be derived by,

$$\tilde{D}_{pq}^n = \sum_{i=1}^{n-1} (\delta_{ip} - x_p) x_i M_i \left(\frac{\partial \mu_i}{\partial x_q} - \frac{\partial \mu_i}{\partial x_n} \right) \tag{Eq 3}$$

where the Kronecker delta $\delta_{ip} = 1$ when $i = p$ and 0 otherwise, and μ_i is the chemical potential of species i. Upon the proposed relations, the mobility parameters, Q_i^p, ${}^rQ_i^{p,q}$, and ${}^sQ_i^{p,q,v}$, can be numerically assessed by fitting to experimental diffusion coefficients.

2.2 Marker Displacement and Kirkendall Shift

In case of a diffusion couple in a binary $A - B$ system where the partial molar volume is assumed to be constant, the composition varying with the diffusion time t in the diffusion zone can be described by the equation of continuity,

$$\frac{1}{V_\mathrm{m}} \frac{\partial x_B}{\partial t} = -\nabla \left[\frac{\tilde{M}}{V_\mathrm{m}} \nabla [\mu_B - \mu_A] \right] \tag{Eq 4}$$

where V_m is the molar volume and $\tilde{M} = x_A x_B [x_B M_A + x_A M_B]$. Equation 4 can be solved numerically corresponding to different initial conditions and boundary conditions. The solution expresses the form of the concentration profile.

If diffusion occurs by a vacancy mechanism, the nonuniform velocity of the inert markers with respect to the laboratory-fixed frame of reference is dependent on the difference of the intrinsic diffusivities of the species and the composition gradient,[11,15,16]

$$v = V_\mathrm{m}(J_A + J_B) = V_\mathrm{m}(D_B - D_A) \frac{\partial x_B}{\partial z} \tag{Eq 5}$$

where J_A and J_B are the flux of species A and B relative to a lattice-fixed frame, D_A and D_B are the intrinsic diffusivities of species A and B, and z is the distance. When using a reduced distance variable, $\lambda = z/\sqrt{t}$, it reads

$$v = \frac{V_\mathrm{m}(D_B - D_A)}{\sqrt{t}} \frac{\partial x_B}{\partial \lambda} \tag{Eq 6}$$

In a diffusion-controlled interaction, the Kirkendall plane is the only plane that stays at a constant composition during the whole diffusion annealing and moves parabolically in time with a velocity,

$$v_\mathrm{k} = \frac{dz}{dt} = \frac{z_\mathrm{k} - z_{\mathrm{k}0}}{2t} = \frac{z_\mathrm{k}}{2t} \tag{Eq 7}$$

where z_k and z_{k0} (=0) are the positions of the Kirkendall plane at times $t = t$ and $t = 0$, respectively. As a result, it can be graphically determined from the Kirkendall velocity construction, that is, a plot of the velocity of the inert markers as a function of the distance, by finding the intersection between the marker velocity curve (Eq 6) and the straight line (Eq 7).[11,17,18] The lattice plane displacement can be computed from the velocity of the inert markers by integrating

$$\frac{\partial y}{\partial z_0} = \frac{y - 2vt}{z_0} \tag{Eq 8}$$

where z_0 is the position of original location of the markers, and y is the displacement of the markers relative to z_0.

3. Assessment of Atomic Mobility

The thermodynamic descriptions of the systems Co-Ni and Co-Fe were taken from the works of Guillermet.[2,3] The atomic mobilities for the self-diffusions of the fcc Fe and Ni were taken from the work of Jonsson.[14] The assessment of other mobility parameters was carried out within the DICTRA software by an iterative optimization based on minimization of the residuals between the calculated values and the selected experimental diffusion coefficients in literature. The optimization process, for the Co-Ni system, was performed mainly by fitting to the data on tracer diffusion for two components and from those data the interdiffusion coefficient was calculated. The situation for the Co-Fe system is different in that the data on interdiffusion were given a dominant weight in the optimization. The results of the assessed mobilities are listed in Table 1. In

Table 1 Assessed atomic mobilities for the fcc phase of the Co-Ni and Co-Fe binaries

Mobility	Parameter, J/mole	Ref
Mobility of Co		
$Q_{\mathrm{Co}}^{\mathrm{Co}}$	− 301,654 − 70.10*T	This work
$Q_{\mathrm{Co}}^{\mathrm{Fe}}$	− 301,900 − 76.58*T	25, 26
$Q_{\mathrm{Co}}^{\mathrm{Ni}}$	− 284,724 − 69.23*T	This work
$Q_{\mathrm{Co}}^{\mathrm{Co,Ni}}$	− 5000	This work
${}^0Q_{\mathrm{Co}}^{\mathrm{Co,Fe}}$	+ 305,495 − 201.71*T	This work
Mobility of Fe		
$Q_{\mathrm{Fe}}^{\mathrm{Co}}$	− 253,301 − 97.97*T	25
$Q_{\mathrm{Fe}}^{\mathrm{Fe}}$	− 286,000 − 79.55*T	14
${}^0Q_{\mathrm{Fe}}^{\mathrm{Co,Fe}}$	− 63,300 + 48.68*T	This work
Mobility of Ni		
$Q_{\mathrm{Ni}}^{\mathrm{Co}}$	− 315,816 − 57.16*T	This work
$Q_{\mathrm{Ni}}^{\mathrm{Ni}}$	− 287,000 − 69.80*T	14
${}^0Q_{\mathrm{Ni}}^{\mathrm{Co,Ni}}$	+ 9335	This work

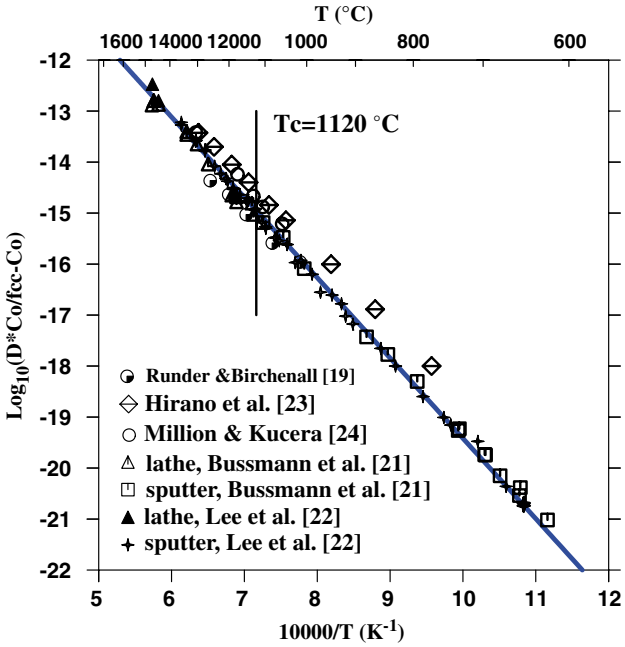

Fig. 1 Arrhenius plot of fcc-Co self-diffusion. The calculated values (solid line) are compared with the experimental points (symbols)

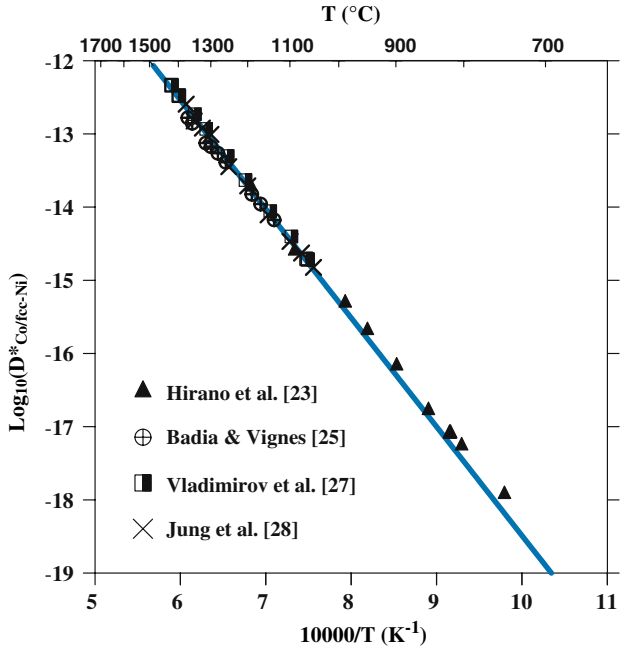

Fig. 2 Arrhenius plot of Co diffusion in fcc-Ni compared with the experimental data (symbols)

the sections that follow, the results of the present assessment are discussed compared with experimental information.

Campbell et al.[5] assessed the atomic mobility for the self-diffusion of fcc-Co and compared it with the early experimental data[19,20] (in fact, the authors misread the Co impurity diffusivity in fcc-Ni[20] as the self-diffusivity in fcc-Co). Only two more recent experimental data[21,22] were considered in the present work. Figure 1 shows an Arrhenius plot of fcc-Co self-diffusion. Excellent agreement is obtained between the calculated and experimental values over a very wide temperature range,[21,22] whereas two other earlier experimental data appear remarkably large, especially in the low-temperature range.[23,24]

3.1 The Co-Ni System

3.1.1 Tracer Diffusivity. In Fig. 2, the calculated Co impurity diffusion in fcc-Ni compares favorably with all available experimental data.[23,25,27,28] The experimental data for the impurity diffusivity of Ni in fcc-Co lie within a narrow band,[23,25,29-31] as shown by the Arrhenius plot of the Ni diffusion in fcc-Co in Fig. 3. Appreciable care was given to the selection of those data. The assessed result (solid line in Fig. 3) was mainly based on the work of Million and Kucera[31] and a recommended value at 1100 °C, supplemented with a compromise made among three measurements.[25,29,30] The recommended value is 1.0×10^{-15} (m^2/s), and was derived from a wide variety of experimental measurements either by extrapolating or eye guide.[30-35]

The calculated tracer diffusivity of Co in the Co-Ni binary alloys is shown to be dependent on the Ni content in

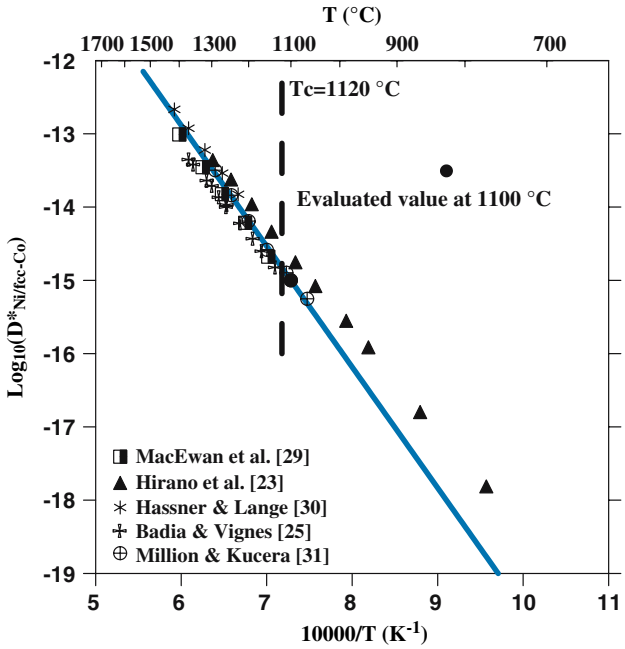

Fig. 3 Arrhenius plot of Ni diffusion in fcc-Co compared with the experimental data (symbols)

Fig. 4 and is in good agreement with the experimental data.[23] The data measured by Million and Kucera[24] exhibit appreciable scatter and, therefore, were excluded from the assessment procedure in this work. Note that an arbitrarily chosen scaling factor S has been added in Fig. 4

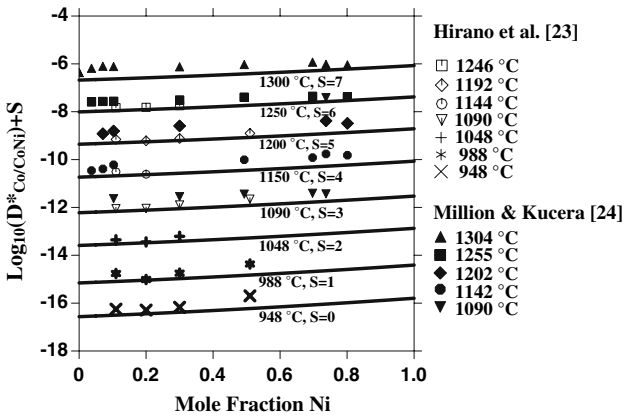

Fig. 4 Calculated tracer diffusivity of Co in the fcc Co-Ni binary alloys. Symbols are from the experimental measurements. An arbitrarily chosen scaling factor S is added to clearly represent the data at different temperatures

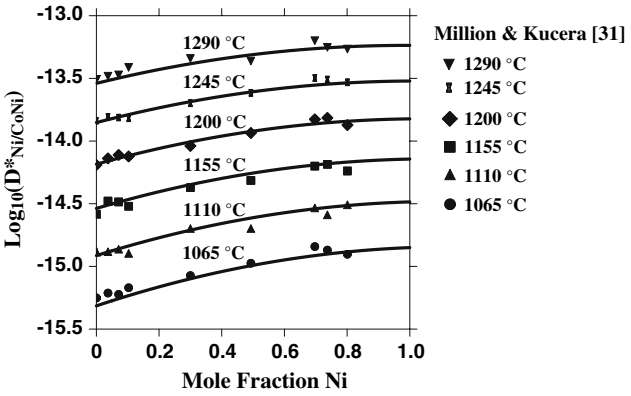

Fig. 5 Calculated tracer diffusivity of Ni in the fcc Co-Ni binary alloys. Symbols are from the experimental measurements

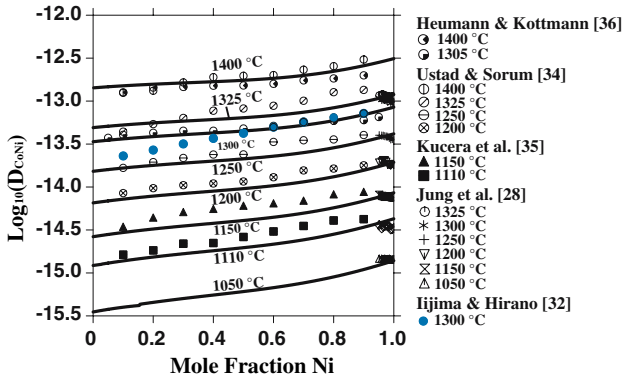

Fig. 6 Calculated interdiffusion coefficients of the fcc Co-Ni binary alloys. Symbols are from the experimental measurements

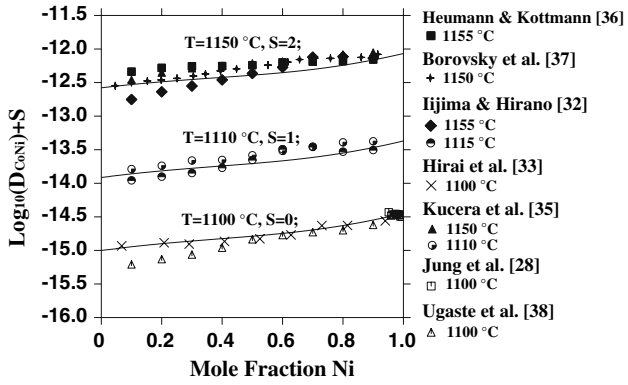

Fig. 7 Calculated interdiffusion coefficients of the fcc Co-Ni binary alloys at 1150, 1110, and 1100 °C. Symbols are from the experimental measurements. An arbitrarily chosen scaling factor S has been added to separate the data at different temperatures

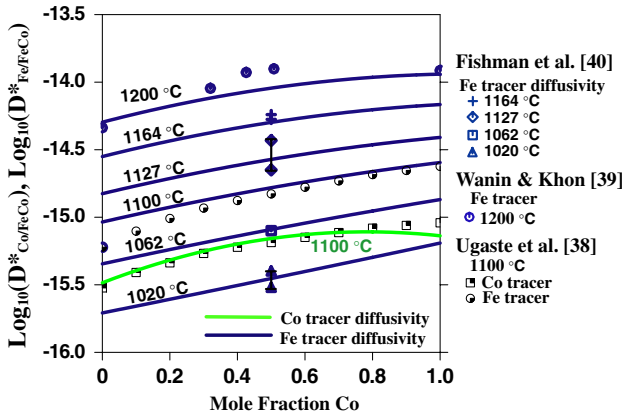

Fig. 8 Calculated tracer diffusivities of Co and Fe in the fcc Co-Fe binary alloys. Symbols are from the experimental measurements

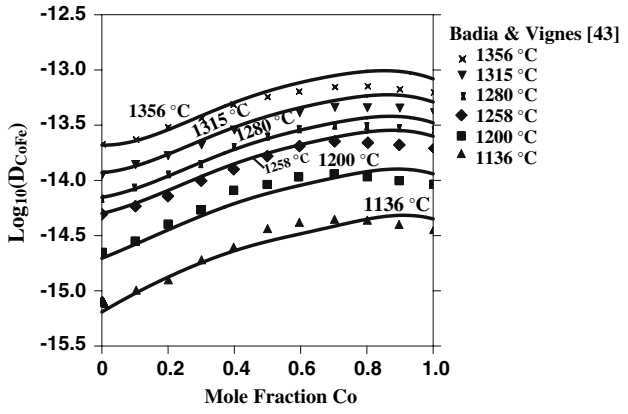

Fig. 9 Calculated interdiffusion coefficients of the fcc Co-Fe binary alloys. Symbols are from the experimental measurements

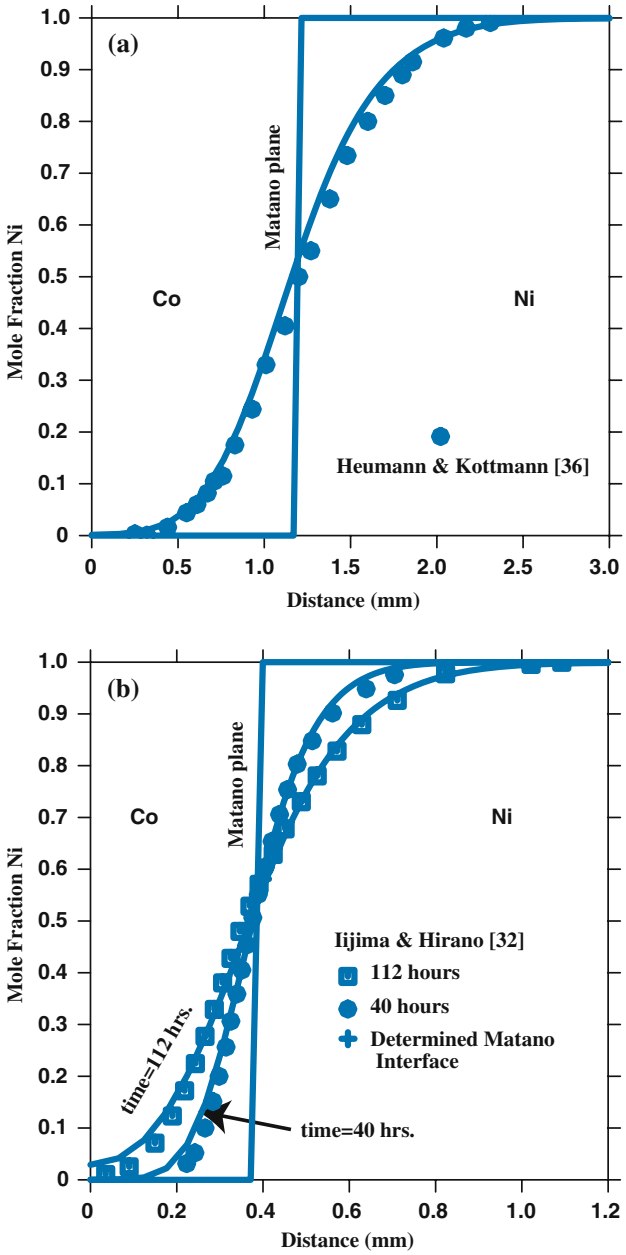

Fig. 10 Calculated concentration profiles for the Co/Ni diffusion couples (a) at 1305 °C for 485 h (b) at 1300 °C for 40 and 112 h. Symbols are from the experimental measurement

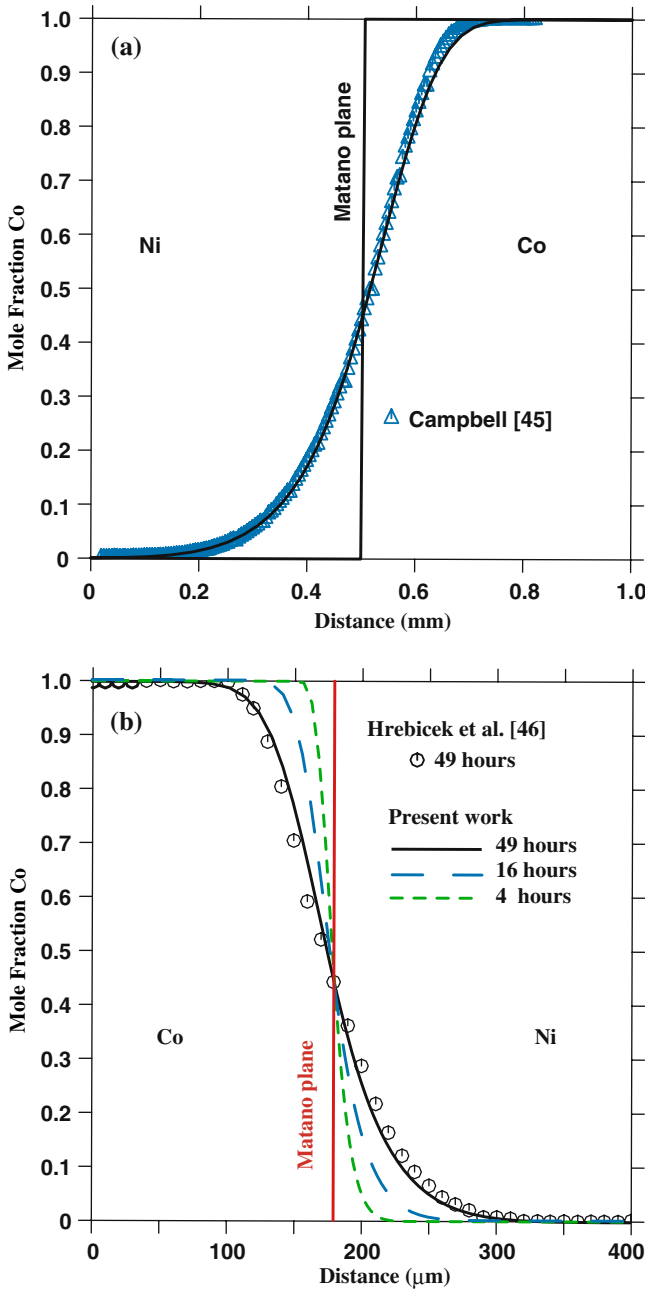

Fig. 11 Calculated concentration profiles for the Co/Ni diffusion couples (a) at 1100 °C for 1000 h (b) at 1150 °C for 4, 16, and 49 h. Symbols are from the experimental measurements

to separate the data at different temperatures. Without it, many symbols at different temperatures would lie too close together to distinguish clearly. Precise agreement may be observed in Fig. 5 for the tracer diffusivity of Ni in the binary alloys between the calculated and measured values,[31] where the curves show a convex shape. This shape is inverse to that of the T_0 line of the binary Co-Ni phase diagram.[2]

3.1.2 Interdiffusion Coefficient. The calculated interdiffusion coefficients of the Co-Ni binary alloys are given in Fig. 6 with the experimental data shown for comparison. Figure 7 presents an enlargement of the temperature span from 1100 to 1150 °C. It is apparent that the data obtained by different authors[28,32,33,35-38] differ markedly; only two of them[28,33] extrapolate to reasonable impurity diffusivities of Ni in fcc-Co and of Co in fcc-Ni, which were retained in the assessment of the mobility parameters.

3.2 The Co-Fe System

3.2.3 Tracer Diffusivity. The mobility of the impurity diffusion of Co in fcc-Fe was taken from the data of Badia and Vignes[25] and Suzuoka,[26] and that of Fe in fcc-Co was

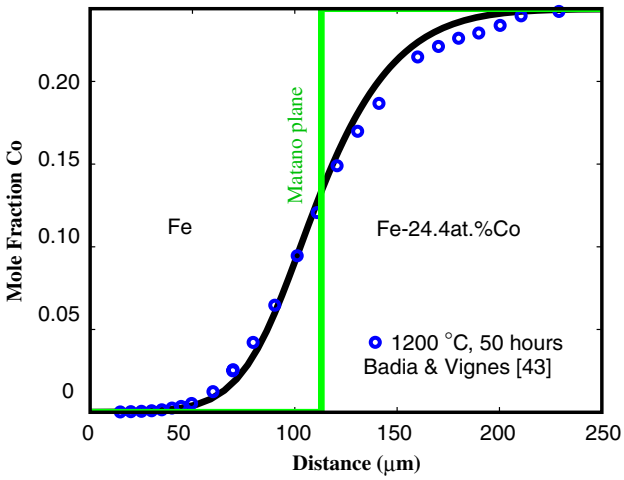

Fig. 12 Calculated concentration profile for the Fe/Fe-24.4 at.%Co incremental couple at 1200 °C for 50 h in comparison with the experimental data

given by Badia and Vignes[25] The variation of the Fe and Co tracer diffusions in the Co-Fe binary alloys with composition were more or less in accord with each other among three measurements,[38-40] but in substantial disagreement with the others.[41,42] The former[38-40] are believed to be more reliable because those data behave in better accord with the proposed impurity diffusion rates,[25,26] and were therefore used to assess the interaction parameters of the Co-Fe atomic mobility. However, closer inspection revealed that the Co tracer diffusivity measured by Fishman et al.[40] does not work well with the interdiffusion rate measured by Badia and Vignes[43] As a result, this set of the Co tracer diffusivity was finally excluded from the assessment. The calculated tracer diffusivities are compared with the measured data in Fig. 8.

3.2.4 Interdiffusion. As seen from Fig. 9, the calculated interdiffusion coefficient compares favorably with the experimental values of Badia and Vignes.[43] Two other sets of data were not given because one appears substantially large[38] and the other describes an overcomplex variation of interdiffusion coefficients with composition.[44]

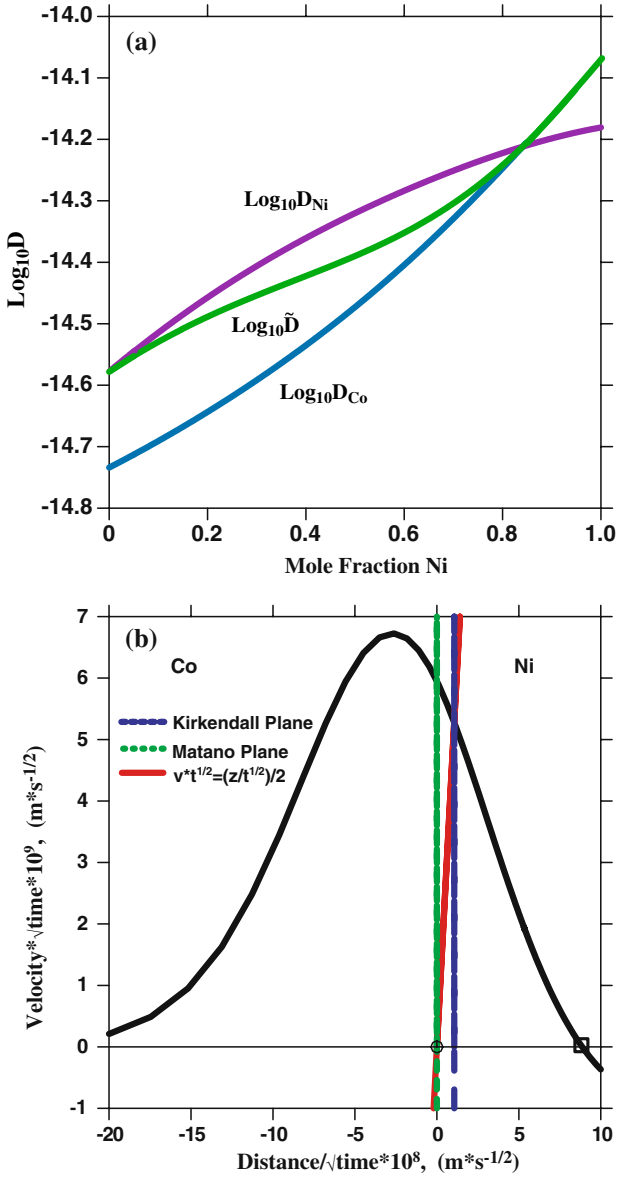

Fig. 13 (a) Intrinsic diffusivities and interdiffusion versus the Ni mole fraction at 1150 °C. (b) Kirkendall velocity construction for the Co/Ni diffusion couple at 1150 °C

4. Diffusion Simulations

Evaluation of the assessed diffusion mobility not only includes comparison with the experimental diffusion coefficients, but also comparison between the predicted and observed in-depth diffusion behavior resulting from interdiffusion. In conjunction with the CALPHAD-base thermodynamics, solving Eq 4, 6, and 8 numerically with input of the assessed atomic mobility enables prediction of much of the diffusion phenomena during a diffusion-couple experiment.

4.1 Concentration Profile of Diffusion Couple

Diffusion simulation has been set up to model a number of semi-infinite Co/Ni and Fe/Fe-Co diffusion-couple experiments under different initial conditions and heat treatment processes. Figure 10 shows the calculated concentration profiles of two Co/Ni diffusion couples after annealing at 1305 °C for 485 h (Fig. 10a) and at 1300 °C for 40 and 112 h (Fig. 10b), respectively. The calculations are in reasonable agreements with the measured curves.[32,36] However, minor discrepancy was observed on the Co-side of the diffusion couple in Fig. 10(b). This can be understood by looking back to Fig. 6, where an underestimated interdiffusion coefficient (the light symbols) measured by Iijima and Hirano[32] was observed in the Co-rich content at 1300 °C.

Figure 11 shows the concentration profiles of two other Co/Ni couples after annealing at 1100 °C for 1000 h

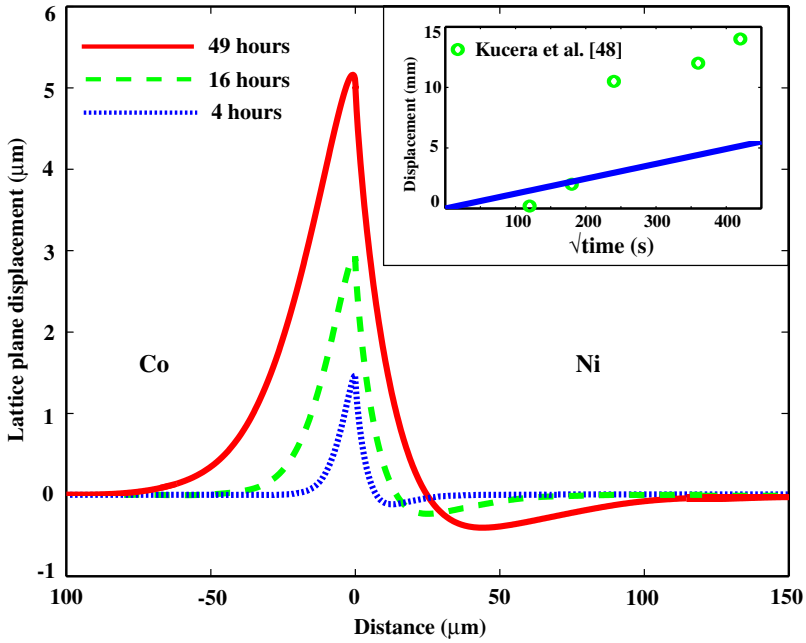

Fig. 14 Lattice plane displacement of the Co/Ni diffusion couples after annealing for 4, 16, and 49 h at 1150 °C as a function of the initial lattice position. The inset shows the Kirkendall marker displacement versus the square root of the diffusion time at 1150 °C. Symbols are from the experimental measurement

(Fig. 11a) and at 1150 °C for 4, 16, and 49 h (Fig. 11b). Precise representation is achieved for both couples.[45,46] It should be noted that, rather than using the new technique for database evaluation proposed by Campbell,[45] but fixing the relevant impurity diffusivities by rigorously fitting to the measured data, the present authors have obtained better calculated concentration profile without allowing any arbitrarily given impurity diffusivity.

Figure 12 shows the calculated concentration profile of the Fe/Fe-20 at.%Co incremental couple annealing at 1150 °C for 50 h. The agreement with the measured curve is satisfactory at the Fe side of the couple,[43] but not so good at the incremental alloy side. This discrepancy results from the fixed impurity diffusivity of Fe in fcc-Co.

4.2 Kirkendall Velocity Construction and Marker Displacement

As stated previously, the velocity of the inert markers can be determined from the knowledge of intrinsic diffusivities and the composition gradient at the marker position. Figure 13(a) shows the variation of two intrinsic diffusivities D_{Co} and D_{Ni} with compositions, which take slightly different forms and cross each other at the Ni-rich side. Figure 13(b) illustrates the Kirkendall velocity construction for the Co/Ni diffusion couple annealing at 1150 °C. Note that the reduced velocity curve $v\sqrt{t}$ intersects the straight line $vt = z/2\sqrt{t}$ (determined by Eq 7) at a point with a negative gradient. As a result, there is a stable Kirkendall plane for the Co/Ni couple at 1150 °C; that is, the Kirkendall marker remains sharply concentrated. This fact has been expected experimentally.[32,47] It should be also noted that the point with a zero velocity, marked by the square symbol in Fig. 13(b), corresponds to the position where the two intrinsic diffusivities are identical, see Fig. 13(a). The Ni-Pd diffusion couple was found to have a similar feature on the microstructural stability of the Kirkendall plane.[11,48]

Integration of Eq 8 yields the lattice plane displacement as a function of the initial lattice position relative to the Matano plane, see Fig. 14 for the Co/Ni diffusion couple annealed at 1150 °C for 4, 16, and 49 h, respectively. As can be seen, the shift of the Kirkendall marker is as small as about 5.2 μm toward the Ni side of the couple after annealing for 49 h. This is in good accord with the finding that the Kirkendall markers move toward the Ni side but were almost immobile.[32,36,38] The displacement of the Kirkendall plane is plotted in the inset of Fig. 14 as a function of the square root of the diffusion time. Appreciable discrepancies were observed for the long diffusion times, which were believed to arise from two critical errors associated with the displacement measurement mentioned already by Kucera et al.[47] The first is the mechanical pressing of the inert markers into the Ni side prior to diffusion annealing. This deformation has to be removed to gain genuine displacement by a way used by Van Dal et al.[48] The second is the errors in the distance measurement of the initial markers, and this effect could most probably lead to surprisingly large displacement.[47]

Figure 15(a) shows the calculated intrinsic diffusivities and interdiffusion coefficients of the Co-Fe binary system at 1100 °C. Figure 15(b) gives the Kirkendall velocity construction for the Co-Fe diffusion couple annealing at 1100 °C. Note that it also exhibits an intersection with a negative gradient, and thus a stable Kirkendall plane occurs for the Co/Fe couple at 1100 °C. The calculated shift and

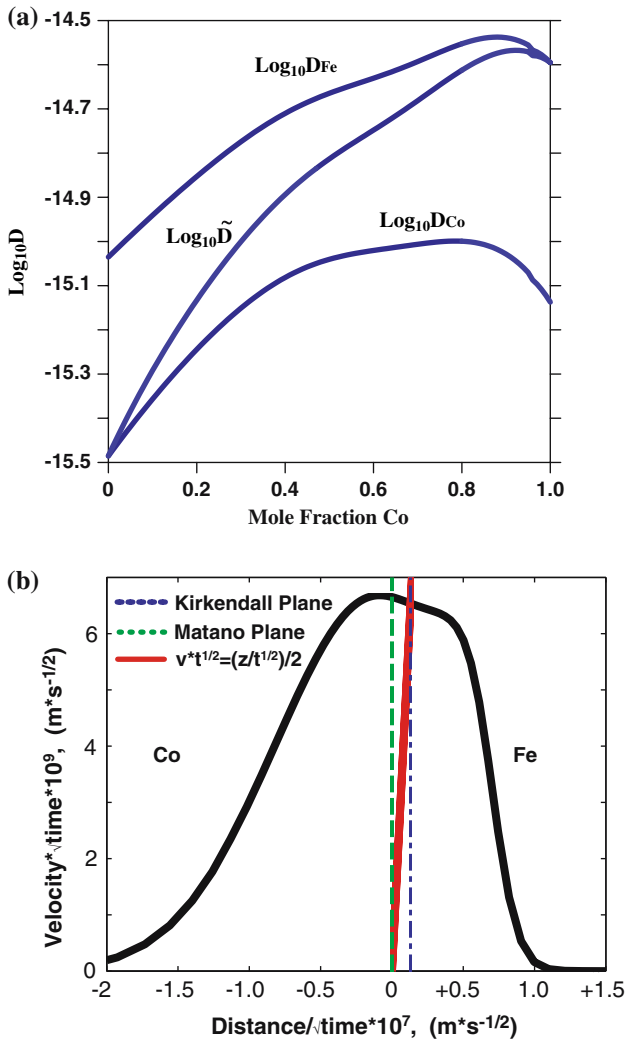

Fig. 15 (a) Intrinsic diffusivities and interdiffusion coefficients versus the mole fraction of Co at 1100 °C. (b) Kirkendall velocity construction for the Co/Fe diffusion couple at 1100 °C

composition of the Kirkendall plane are 11 μm and 46 at.% Co for the diffusion couple after annealing for 196 h, which compare fairly with the experimental values, 16 μm and 42 at.% Co.[38]

5. Conclusion

The atomic mobilities for the fcc phase of the Co-Ni and Co-Fe binaries have been assessed by fitting to the evaluated experimental diffusion coefficients. The developed mobility database, in conjunction with CALPHAD-base thermodynamics, has been used to successfully model a number of semi-infinite Co/Ni and Fe/Co diffusion-couple experiments. The concentration profiles have been well represented, and the interesting details concerning the microstructural stability of the Kirkendall plane and the lattice plane displacement have been predicted. The general agreement has been obtained by comprehensive comparisons between the calculated and experimental data.

Acknowledgments

This work was supported by CREST, Japan Science and Technology Agency. YC gratefully acknowledges to the 21st century COE program for financial support.

References

1. J. Sato, T. Ohmori, I. Ohnuma, R. Kainuma, and K. Ishida, Cobalt-Base High-Temperature Alloys, *Science*, 2006, **312**, p 90-91
2. A.F. Guillermet, Assessment of the Thermodynamic Properties of the Ni-Co System, *Z. Metallkd.*, 1987, **78**(9), p 639-647
3. A.F. Guillermet, Critical Evaluation of the Thermodynamic Properties of the Fe-Co System, *High Temp. High Press*, 1988, **19**(5), p 477-499
4. J. Sato, K. Oikawa, R. Kainuma, and K. Ishida, Experimental Verification of Magnetically Induced Phase Separation in αCo Phase and Thermodynamic Calculations of Phase Equilibria in the Co-W System, *Mater. Trans.*, 2005, **46**(6), p 1199-1207
5. C.E. Campbell, W.J. Boettinger, and U.R. Kattner, Development of a Diffusion Mobility Database for Ni-Base Superalloys, *Acta Mater.*, 2002, **50**(4), p 775-792
6. C.E. Campbell, J.-C. Zhao, and M.F. Henry, Comparison of Experimental and Simulated Multicomponent Ni-Base Superalloy Diffusion Couples, *J. Phase Equilibria Diffusion*, 2004, **25**(1), p 6-15
7. J.Z. Zhu, L-Q Chen, J. Shen, and V. Tikare, Coarsening Kinetics from a Variable-Mobility Cahn-Hilliard Equation: Application of a Semi-implicit Fourier Spectral Method, *Phys. Rev. E*, 1999, **60**(4), p 3564-3572
8. J.Z. Zhu, Z.K. Liu, V. Vaithyanathan, and L.-Q. Chen, Linking Phase-Field Model to CALPHAD: Application to Precipitate Shape Evolution in Ni-Base Alloys, *Scr. Mater.*, 2002, **46**(5), p 401-406
9. J.Z. Zhu, T. Wang, A.J. Ardell, S.H. Zhou, Z.-K. Liu, and L.-Q Chen, Three-Dimensional Phase-Field Simulations of Coarsening Kinetics of γ′ Particles in Binary Ni-Al Alloys, *Acta Mater.*, 2004, **52**(9), p 2837-2845
10. A. Borgenstam, A. Engstrom, L. Hoglund, and J. Agren, DICTRA, a Tool for Simulation of Diffusional Transformations in Alloys, *J. Phase Equilibria Diffusion*, 2000, **21**(3), p 269-280
11. L. Hoglund and J. Agren, Analysis of the Kirkendall Effect, Marker Migration and Pore Formation, *Acta Mater.*, 2001, **49**(8), p 1311-1317
12. H. Strandlund and H. Larsson, Prediction of Kirkendall Shift and Porosity in Binary and Ternary Diffusion Couples, *Acta Mater.*, 2004, **52**(15), p 4695-4703
13. J.O. Andersson and J. Agren, Models for Numerical Treatment of Multicomponent Diffusion in Simple Phases, *J. Appl. Phys.*, 1992, **72**(4), p 1350-1355
14. B. Jonsson, Ferromagnetic Ordering and Diffusion of Carbon and Nitrogen in bcc Cr-Fe-Ni Alloys, *Z. Metallkd.*, **85**(7), p 498-501
15. J.F. Cornet and D. Calais, Etude de L'Effet Kirkendall D'Apres les Equations de Darken, *J. Phys. Chem. Solid.*, 1972, **33**(9), p 1675-1684, in French
16. N.S. Kulkarni, C.V. Iswaran, and R.T. DeHoff, Intrinsic Diffusion Simulation for Single-Phase, Multicomponent Systems, *Acta Mater.*, 2005, **53**(15), p 4097-4110

17. M.J.H van Dal, A.M. Gusak, C. Cserhati, A.A. Kodentsov, and F.J.J van Loo, Microstructural Stability of the Kirkendall Plane in Solid-State Diffusion, *Phys. Rev. Lett.*, 2001, **86**(15), p 3352-3355
18. M.J.H. van Dal, A.M. Gusak, C. Cserhati, A.A. Kodentsov, and F.J.J. van Loo, Spatio-Temporal Instabilities of the Kirkendall Marker Planes During Interdiffusion in β′-AuZn, *Philos. Mag. A*, 2002, **82**(5), p 943-954
19. R.C. Ruder and C.E. Birchenall, Cobalt Self-Diffusion-A Study of the Method of Decrease in Surface Activity, *Trans. AIME*, 1951, **191**(2), p 142-146
20. B. Million and J. Kucera, Diffusion von Kobalt in Ni-Co-Legierungen bei Temperaturen bis 1000°C, *Z. Metallkd.*, 1972, **63**(8), p 484-489, in German
21. W. Bussmann, Ch. Herzig, W. Rempp, K. Maier, and H. Mehrer, Isotope Effect and Self-Diffusion in Face-Centered Cubic Cobalt, *Phys. Stat. Sol. (a)*, 1979, **56**(1), p 87-97, in German
22. C.-G. Lee, Y. Iijima, and K. Hirano, Self-Diffusion and Isotope Effect in Face-Centred Cubic Cobalt, *Defect Diffusion Forum*, 1993, **95-98**, p 723-728
23. K. Hirano, R.P. Agarwala, B.L. Averback, and M. Cohen, Diffusion in Cobalt-Nickel Alloys, *J. Appl. Phys.*, 1962, **33**(10), p 3049-3054
24. B. Million and J. Kucera, Concentration Dependence of Diffusion of Cobalt in Nickel-Cobalt, *Acta Met.*, 1969, **17**(3), p 339-344
25. M. Badia and A. Vignes, Iron, Nickel and Cobalt Diffusion in Transition Metals of Iron Group, *Acta Met.,*, 1969, **17**(2), p 177-187, in French
26. T. Suzuoka, Lattice Diffusion and Grain Boundary Diffusion of Cobalt in γ-Iron, *Trans. JIM*, 1961, **2**(3), p 176-182
27. B. Vladimirov, V.N. Kaygorodov, S.M. Klotsman, and I.S. Trakhtenberg, Volumetrical Diffusion of Cobalt and Tungsten in Nickel, *Fiz. Met. Metalloved.*, 1978, **46**(6), p 1232-1239, in Russian
28. S.B. Jung, T. Yamane, Y. Minamino, K. Hirano, H. Araki, and S. Saji, Interdiffusion and its Size Effect in Nickel Solid-Solutions of Ni-Co, Ni-Cr and Ni-Ti Systems, *J. Mater. Sci. Lett.*, 1992, **11**(20), p 1333-1337
29. J.R. MacEwan, J.U. MacEwan, and L. Yaffe, Diffusion of Ni-63 in Iron, Cobalt, Nickel, and Iron-Nickel Alloys, *Canad. J. Chem.*, 1959, **37**(10), p 1629-1636
30. A. Hassner and W. Lange, Volumenselbstdiffusion in Kobalt-Nickel-Legierungen, *Phys. Stat. Sol.*, 1965, **8**(1), p 77-91, in German
31. B. Million and J. Kucera, Concentration Dependence of Nickel Diffusion in Nickel-Cobalt Alloys, *Czech. J. Phys.*, 1971, **21**(2), p 161-171
32. Y. Iijima and K. Hirano, Interdiffusion in Cobalt-Nickel Alloys, *J. Jpn. Inst. Met.*, 1971, **35**(5), p 511-517, in Japanese
33. Y. Hirai, Y. Tasaki, and M. Kosaka, A Study on the Friction-Welded Diffusion Couples-Chemical Diffusion of Co-Ni Alloy at 1000°C, *Nagoya Kogyo Gijutso Shikenso Hokoku*, 1973, **22**(4), p 125-131, in Japanese
34. T. Ustad and H. Sorum, Interdiffusion in Fe-Ni, Ni-Co, and Fe-Co Systems, *Phys. Stat. Sol. (a)*, 1973, **20**(1), p 285-294
35. J. Kucera, K. Ciha, and K. Stransky, Interdiffusion in Co-Ni System-Concentration Penetration Curves and Interdiffusion Coefficients, *Czech. J. Phys. B*, 1977, **27**(7), p 758-768
36. Th. Heumann and A. Kottmann, Uber den Ablauf der Diffusionsvorgange in Substitutionsmischkristallen, *Z. Metallkd.*, 1953, **44**(4), p 139-154, in German
37. I.B. Borovskiy, I.D. Marchukova, and Yu.E. Ugaste, Local X-ray Spectranalysis of Mutual Diffusion in Binary Systems Forming a Continuuous Series of Solid Solutions-Systems Fe-Ni Ni-Co Ni-Pt and Co-Pt, *Phys. Met. Metallogr.*, 1967, **24**(3), p 436-441, in Russian
38. Yu.E. Ugaste, A.A. Kodentsov, and F. van Loo, Compositional Dependence of Diffusion Coefficients in the Co-Ni, Fe-Ni, and Co-Fe Systems, *Phys. Met. Metallogr.*, 1999, **88**(6), p 598-604
39. M. Wanin and A. Khon, Determination by Tracer Technics of Iron and Nickel Diffusion Coefficients in Iron-Nickel Alloys and of Iron and Cobalt in Iron-Cobalt Alloys, *C.R. Acad. Sci. C*, 1968, **267**(23), p 1558-1561, in French
40. S.G. Fishman, D. Gupta, and D.S. Lieberman, Diffusivity and Isotope-Effect Measurements in Equiatomic Fe-Co, *Phys. Rev. B*, 1970, **2**(6), p 1451-1460
41. T. Hirone, N. Kunitomi, and M. Sakamoto, Diffusion of Cobalt into Iron-Cobalt Alloy, *J. Phys. Soc. Jpn.*, 1958, **13**(8), p 840-844
42. K. Hirano and M. Cohen, Diffusion of Cobalt in Iron-Cobalt Alloys, *Trans. JIM*, 1972, **13**(2), p 96-102
43. M. Badia and A. Vignes, Influence of Structure Changes Produced by Interdiffusion on Interdiffusion Coefficient and Kirkendall Effect, *Rev. Met.*, 1969, **66**(12), p 915-927, in French
44. K. Hirano, Y. Iijima, K. Araki, and H. Homma, Interdiffusion in Iron-Cobalt Alloys, *Trans. ISIJ*, 1977, **17**(4), p 194-203
45. C.E. Campbell, A New Technique for Evaluating Diffusion Mobility Parameters, *J. Phase Equilibria Diffusion*, 2005, **26**(5), p 435-440
46. J. Hrebicek, J. Kucera, and K. Stransky, Determination of Interdiffusion Coefficients in Co-Ni System with Use of Spline Functions, *Czech. J. Phys. B*, 1975, **25**(10), p 1181-1191
47. J. Kucera, K. Ciha, and K. Stransky, Interdiffusion in Co-Ni System-III-Intrinsic Diffusion Coefficients, *Czech. J. Phys. B*, 1977, **27**(9), p 1049-1059
48. M.J.H. van Dal, M.C.L.P. Pleumeekers, A.A. Kodentsov, and F.J.J. van Loo, Intrinsic Diffusion and Kirkendall Effect in Ni-Pd and Fe-Pd Solid Solutions, *Acta Mater.*, 2000, **48**(2), p 385-396